

# Long-Term Rescue of a Lethal Inherited Disease by Adeno-Associated Virus–Mediated Gene Transfer in a Mouse Model of Molybdenum-Cofactor Deficiency

S. Kügler, R. Hahnewald, M. Garrido, and J. Reiss

Molybdenum cofactor (MoCo) deficiency is a progressive neurological disorder that inevitably leads to early childhood death because of the lack of any effective therapy. In a mouse model of MoCo deficiency type A, the most frequent form of this autosomal recessively inherited disease, the affected animals show the biochemical characteristics of sulphite and xanthine intoxication and do not survive >2 wk after birth. We have constructed a recombinant-expression cassette for the gene *MOCS1*, which, via alternative splicing, facilitates the expression of the proteins MOCS1A and MOCS1B, both of which are necessary for the formation of a first intermediate, cyclic pyranopterin monophosphate (cPMP), within the biosynthetic pathway leading to active MoCo. A recombinant adeno-associated virus (AAV) vector was used to express the artificial *MOCS1* minigene, in an attempt to cure the lethal *MOCS1*-deficient phenotype. The vector was used to transduce *Mocs1*-deficient mice at both 1 and 4 d after birth or, after a pretreatment with purified cPMP, at 40 d after birth. We report here that all *Mocs1*-deficient animals injected with a control AAV-enhanced green fluorescent protein vector died ~8 d after birth or after withdrawal of cPMP supplementation, whereas AAV-*MOCS1*-transduced animals show significantly increased longevity. A single intrahepatic injection of AAV-*MOCS1* resulted in fertile adult animals without any pathological phenotypes.

Molybdenum cofactor (MoCo) is essential for the function of the mammalian enzymes aldehyde oxidase, xanthine dehydrogenase, and sulphite oxidase.<sup>1</sup> The biosynthetic pathway leading to MoCo requires several enzymes encoded by the genes *MOCS1*, *MOCS2*, *MOCS3*, and *GEPH*.<sup>2</sup> Mutations in any of these genes abolish formation of active MoCo, leading to the pleiotropic loss of all MoCo-dependent enzymes and resulting in elevated levels of cytotoxic sulphite and xanthine. Elevated sulphite levels cause progressive neuronal loss and death before adolescence in affected patients. No curative treatment is currently available. All forms of this disease are inherited autosomal recessively, and most patients harbor mutations in the gene *MOCS1*. Loss of *MOCS1* function—MoCo deficiency type A (MIM 252150)—results in the inability to catalyze the first step in MoCo biosynthesis, which leads to precursor Z. Precursor Z has recently been renamed “cyclic pyranopterin monophosphate” (cPMP).<sup>1</sup>

We described elsewhere the construction of a murine model for MoCo deficiency type A,<sup>3</sup> which has no detectable residual *Mocs1* mRNA levels. Using this null mutant animal model, we demonstrated the feasibility of a substitution therapy with cPMP purified from *Escherichia coli* extracts.<sup>4</sup> However, this substitution therapy required frequent and lifelong injections of cPMP because of the short half-life of both the molecule and the MoCo-dependent enzymes. Furthermore, the production of purified cPMP on

a scale sufficient for the treatment of patients has proven difficult (G. Schwarz, personal communication).

We therefore set out to explore the possibilities of somatic gene therapy for MoCo deficiency. Since the use of integrating viruses is potentially associated with genotoxicity,<sup>5</sup> we used AAV vectors (the genome of which is maintained episomally) to deliver the *MOCS1* gene into *Mocs1*-deficient mice. This approach required the construction of an expression cassette suitable for the long-term expression of both MOCS1A and MOCS1B, as well as for packaging into a recombinant AAV vector.

We report here that a single injection of an AAV carrying the *MOCS1* expression cassette is sufficient to suppress the severe MoCo-deficiency phenotype and results in fertile adult animals. This study, to our knowledge, is the first reported to use curative gene therapy in a mouse model of an inherited metabolic disease that has complete mortality in early childhood and, thus, represents an important step forward in the therapy for patients with previously incurable conditions.

## Material and Methods

### Construction of the MOCS1A/1B Expression Cassette

The enhancer region of the cytomegalovirus (CMV) promoter was amplified from a template plasmid (pCURE) constructed previously in our laboratory. The promoter region of the human  $\beta$ -actin gene was cloned from a BAC (ResGen). The polyadenylation (polyA) signal of the bovine growth hormone (BGH) gene was

From the Neurologische Universitätsklinik, Abteilung Allgemeine Neurologie, OFG Research Center for the Molecular Physiology of the Brain (CMPB) (S.K.; M.G.), and Institut für Humangenetik der Universität Göttingen (R.H.; J.R.), Göttingen, Germany

Received September 26, 2006; accepted for publication November 20, 2006; electronically published December 19, 2006.

Address for correspondence and reprints: Dr. J. Reiss, Institut für Humangenetik der Universität Göttingen, Heinrich-Düker-Weg 12, D-37073 Göttingen, Germany. E-mail: jreiss@gwdg.de

*Am. J. Hum. Genet.* 2007;80:291–297. © 2006 by The American Society of Human Genetics. All rights reserved. 0002-9297/2007/8002-0009\$15.00

amplified from the plasmid pCURE. Combined with a kanamycin resistance gene (from pACYC) and an origin of replication (from pUC9), these elements form the plasmid pCURE2, with a unique *NotI*-cloning site between the promoter and polyA signal.

Into this *NotI* site, the “Reiss variant” of the human *MOCS1* cDNA<sup>6</sup> was inserted, and, by the use of various restriction sites, the complete intron 9 of the human *MOCS1* gene was first inserted between exons 9 and 10 and was subsequently deleted to a final size of 0.7 kbp, leaving 5′ and 3′ splice sites and the branch-point region unchanged. The resulting plasmid, pRitalX, was amplified in *E. coli* cells, which confirmed a functional kanamycin resistance gene and origin of replication. All other parts of the final plasmid were completely sequenced to exclude PCR errors, mutations, or cloning artifacts. The expression cassette has a total size of 3.6 kbp (fig. 1), and the primary transcript (with a size-reduced intron 9) has a size of 2.8 kbp.

### Establishment of a Transgenic Mouse Strain

The plasmid pRitalX was linearized by a restriction digest of a unique site of the kanamycin resistance gene and was injected into the male pronucleus of fertilized oocytes, which were subsequently reimplanted into a pseudopregnant foster mother. The resulting offspring were tested for the presence of the recombinant human *MOCS1* gene, by PCR analysis of tail-tip DNA, and three positive founder animals were mated with heterozygous *Mocs1*-knockout mice to obtain heterozygous animals (*Mocs1*<sup>+/-</sup>) with additional copies of the *MOCS1* human recombinant transgene (*MOCS1*<sup>human+</sup>). A small portion of the tail biopsy was used for RNA isolation, to confirm transcription and alternative splicing by RT-PCR. Heterozygous *Mocs1*-knockout mice with the additional transgene (*Mocs1*<sup>+/-</sup> and *MOCS1*<sup>human+</sup>) were mated, to obtain homozygous mice without a functional endogenous *Mocs1* gene with the additional transgene (*Mocs1*<sup>-/-</sup> and *MOCS1*<sup>human+</sup>).

### AAV Vector Preparation and Applications

Recombinant AAV particles were generated essentially as described elsewhere,<sup>7,8</sup> with the exception that the AAV-2-based genome was packaged into an AAV-1/2 chimeric capsid, which has been demonstrated to have high transduction efficacy for both liver and muscle.<sup>9</sup> A 50:50 ratio of AAV-1 and AAV-2 packaging plasmids was used for this purpose. Vectors were initially purified by iodixanol gradient centrifugation and were further purified and concentrated by fast-protein liquid chromatography on Heparin affinity columns (Amersham). After extensive dialysis against PBS, vectors were stored at -80°C until they were used. Genome copies were determined by quantitative PCR, and purity of >99% was confirmed by PAGE. Functional titres (transducing units [tu]) were determined by transduction of cultures of primary neurons and revealed a ratio of 1:30 (tu:genomes) for the AAV-enhanced green fluorescent protein (EGFP) vector. Since the AAV-*MOCS1* vector was prepared identically, the same tu:genome ratio was assumed for this construct.

Neonatal mice were injected intrahepatically at 1 d after birth with 10 μl containing 1 × 10<sup>9</sup> tu and, after genotyping, were re-injected at age 4 d with 50 μl containing 3 × 10<sup>9</sup> tu of either AAV-EGFP (*n* = 10) or AAV-*MOCS1* (*n* = 9). For vector application into adolescent mice, we first confirmed that both tail vein and direct intrahepatic injection of 10<sup>10</sup> tu AAV-EGFP in a volume of 100 μl resulted in similar tissue transduction (i.e., gene expression predominantly in hepatocytes). Nineteen *Mocs1*-deficient animals

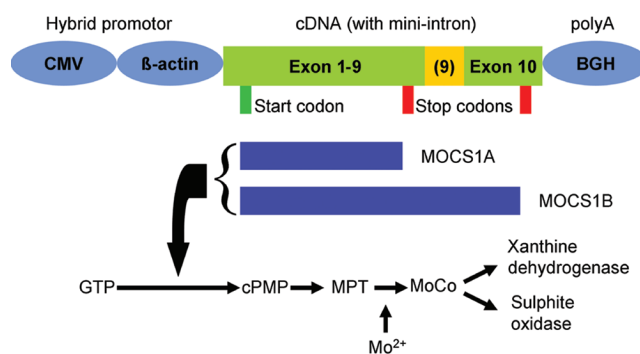


**Figure 1.** Structure of the *MOCS1* expression cassette. The first stop codon, terminating the MOCS1A protein, is partially omitted via alternative splicing, which facilitates expression of the MOCS1B protein. Both proteins are necessary for the formation of cPMP.

were pretreated for 40 d with purified cPMP from *E. coli* (i.e., intrahepatic injection every other day in amounts increasing from 2 μg in the 1st wk to 32 μg in the 5th wk and after). At age 40 d, 9 animals received an intrahepatic injection of 100 μl AAV-*MOCS1* (8 × 10<sup>9</sup> tu), and 10 animals received the same dosage of AAV-EGFP.

### Tissue Preparations

Tissue for expression analysis was prepared from paraformaldehyde-perfused mice, was cryoprotected in sucrose, and was stored at -80° until analysis. Cryostat sections 50 μm thick were prepared for EGFP expression analysis. Confocal pictures were recorded by a Leica SP5 microscope.

### Biochemical Analysis

Urinary sulphite levels were determined semiquantitatively with test strips (Merckoquant sulphite test 1.10013.0001), and total liver molybdopterin (MPT) content and sulphite oxidase activity in liver tissue were measured as described elsewhere.<sup>4</sup>

## Results

### Construction of the *MOCS1* Expression Cassette and Functional Testing in Transgenic Mice

The *MOCS1* expression cassette used in this study is shown in figure 1 and contains (i) a hybrid promoter consisting of a CMV enhancer region and a human β-actin core promoter, (ii) elements of the human *MOCS1* gene: exons 1b, 1c, and 1d (one of three possible splice forms<sup>6</sup>); exons 2–9; a deleted intron 9, which allows for alternative splicing leading to the gene products MOCS1A and MOCS1B; and exon 10, and (iii) the polyA signal of the BGH gene.

Since antibodies to monitor proper expression of both MOCS1A and MOCS1B are not available, functional evaluation of this construct was first achieved by a transgenic approach. The cassette was introduced as a transgene in a wild-type mouse strain (*MOCS1*<sup>human+</sup>), which was then crossed with mice heterozygous for a disrupted endogenous *Mocs1* gene (*Mocs1*<sup>+/-</sup>) to obtain animals heterozygous for the murine *Mocs1* with an additional copy of the

recombinant transgene (*Mocs1*<sup>+/-</sup> and *MOCS1*<sup>human+</sup>). Five matings of 2 animals with *Mocs1*<sup>+/-</sup> and *MOCS1*<sup>human+</sup> resulted in a total of 56 offspring, from which 15 (27%) were genotyped *Mocs1*<sup>-/-</sup>.

Of these 15 animals, 5 carried no recombinant transgene (*MOCS1*<sup>human-</sup>) and died at age 4–12 d. Ten animals carried the recombinant transgene on a double-knockout background (*Mocs1*<sup>-/-</sup> and *MOCS1*<sup>human+</sup>) and developed without a detectable phenotype. They were visually indistinguishable from their littermates with an endogenous *Mocs1* wild-type allele and showed only marginally elevated sulphite levels (~50 mg/liter) in their urine.

At age 43 d, two animals with *Mocs1*<sup>-/-</sup> and *MOCS1*<sup>human+</sup> were sacrificed, and the subsequent autopsy showed normal development of all organs. Biochemical analysis of liver tissue revealed a sulphite oxidase activity of ~50% of the wild-type level (fig. 2*d*). By the time this article was prepared, the remaining eight mice all showed no symptoms of MoCo deficiency and were older than 12 mo. We interpret these results, together with data published elsewhere, to indicate stable expression of a functional transgene.<sup>4</sup>

### Tissue-Transduction Properties of the Recombinant AAV Vector

cPMP is a small molecule that can diffuse from cells in which it is synthesized to neighboring cells, and in which it activates sulphite oxidase, xanthine dehydrogenase, and aldehyde oxidase.<sup>10</sup> This diffusion allows for organwide supply of cPMP by delivery of the *MOCS1* gene to a limited number of cells. The liver is the organ mainly involved in detoxification of sulphite by sulphite oxidase.<sup>11</sup> Thus, gene transfer of the *MOCS1* gene is primarily aimed at hepatocyte transduction. To trace expression of the recombinant AAV vector, *MOCS1* was replaced by the fluorescent reporter EGFP. This AAV-EGFP vector was injected intravenously or intrahepatically into adolescent mice or intrahepatically into newborn mice.

In adult mice, injection of 1 × 10<sup>10</sup> tu AAV-EGFP, either directly into the liver or intravenously into the tail vein, resulted in almost complete transduction of hepatocytes (fig. 3*a* and 3*e*). Single injections were sufficient to transduce hepatocytes throughout the adult liver in all three liver lobes, as assayed 4 wk after injection. Very little trans-

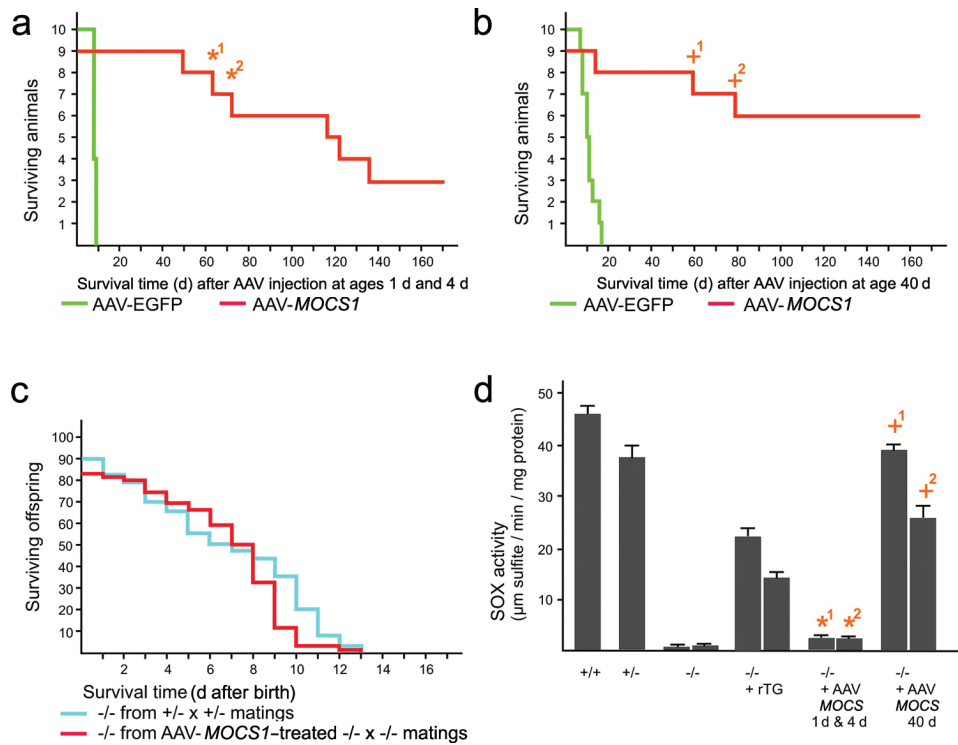


**Figure 2.** Survival and enzymatic activity of *Mocs1*-deficient mice with or without treatment. Group 1 (*a*) was injected with AAV-*MOCS1* (AAV-EGFP as control) on postnatal days 1 and 4. Group 2 (*b*) was pretreated with cPMP as described elsewhere<sup>4</sup> until age 40 d and was then injected with recombinant AAV. The untreated offspring (*c*) are the result of four matings of *Mocs1*-deficient mice of group 2 injected with AAV-*MOCS1* or of matings of two heterozygous mice as a control. *d*, Sulphite oxidase (SOX) activity in liver tissue of heterozygous (+/-) and wild-type (+/+) animals, in comparison with that of deficient (-/-) animals with or without AAV-*MOCS1* injections as indicated or carrying an additional recombinant transgene (rTG). One column represents one animal, which was measured in triplicate. Note that the four animals indicated in panels *a* and *b* (two in each) were sacrificed with healthy phenotypes for enzymatic evaluation.



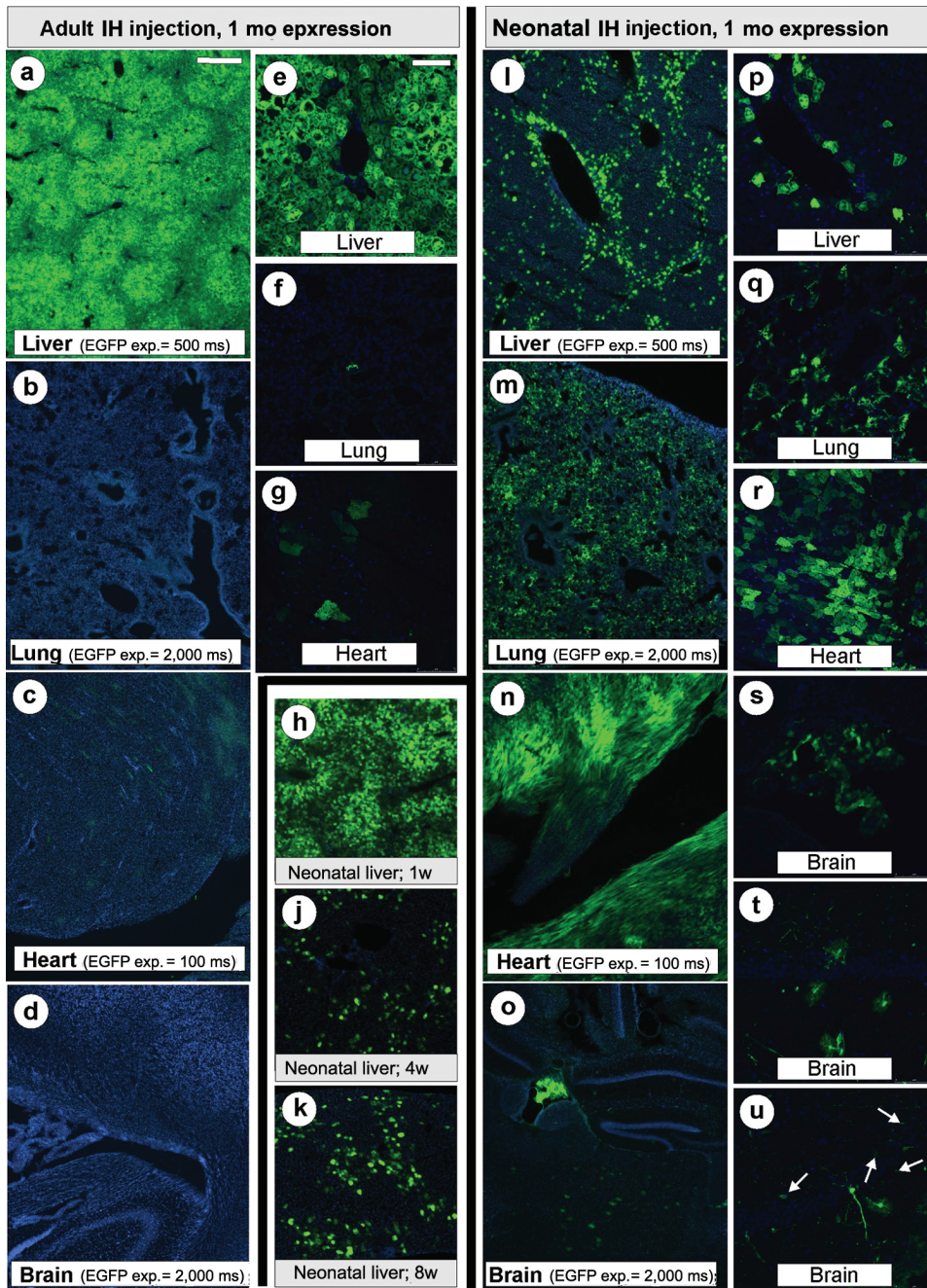


**Figure 3.** Tissue transduction of AAV-EGFP vector after application in adult and neonatal mice. Wide-field (*a-d*, *h-k*, and *l-o*) and confocal (*e-g* and *p-u*) images were obtained from 50- $\mu$ m cryosections. Confocals represent “enlargements” of the respective tissue sections, as recorded by wide-field microscopy. Fluorescence is shown as an overlay of EGFP (*green*) and nuclear DAPI (*blue*) fluorescence. Note that wide-field images were recorded with different exposure (exp.) times for EGFP as indicated. *a-g*, Transduction of adult mice. *h-u*, Transduction of neonatal mice. All tissue was sampled at 1 mo after transduction, with the exception of that shown at 7 d (*h*) and at 2 mo (*k*) after transduction. *u*, Arrows point to small vessels. Scale bars = 400  $\mu$ m (*a-d*, *h-k*, and *l-o*) and 75  $\mu$ m (*e-g* and *p-u*). IH = intrahepatic.



duction was detected in other organs inspected, such as the heart, the lungs, and the brain (fig. 3*b–3d*, 3*f*, and 3*g*). Intravenous and intrahepatic vector application resulted in essentially the same tissue transduction of the AAV vector (not shown).

Since proper tail-vein injection is not possible in newborn mice, only intrahepatic injections with  $5 \times 10^9$  tu AAV-EGFP were performed at age 6 d. Livers analyzed 7 d after vector application showed complete transduction of hepatocytes (fig. 3*h*). The mouse liver increases in weight ~20-fold between the neonatal and adult states. Because of the episomal nature of the AAV-vector genome, the number of transgene-expressing hepatocytes accordingly decreased considerably over time: ~5% of hepatocytes still expressed EGFP 4 wk after transduction of the neonatal liver (fig. 3*j*, 3*l*, and 3*p*). However, 8 wk after transduction, no further decrease of transgene-expressing hepatocytes was detected (fig. 3*k*).

In contrast to vector applications in adult animals, injections into neonatal livers resulted in expression in several tissues. We detected strong EGFP expression in cardiomyocytes throughout the heart muscle (fig. 3*n* and 3*r*) and widespread expression in lung epithelia (fig. 3*m* and 3*q*), although at a considerably lower level than in the liver and heart (note the different exposure times for the recording of EGFP fluorescence in fig. 3). Intriguingly, brain transduction was also observed: inside the ventricles, cells of the choroids plexus showed pronounced EGFP expression (fig. 3*o* and 3*s*), whereas, in the brain parenchyma, several cells with astrocytic morphology expressed EGFP (fig. 3*t*). Small-vessel epithelia and very few neurons also expressed EGFP (fig. 3*u*). As judged by EGFP fluorescence levels, transgene expression remained stable in the transduced tissues, with no detectable decline from 1 to 2 mo after vector application.

Since the above-described AAV-EGFP applications demonstrated divergent tissue tropism between mice injected at the neonatal and adult states, we treated two groups of *Mocs1*-deficient mice at different ages with the AAV-MOCS1 vector.

#### Treatment of Newborn Mice with AAV-MOCS1

Complete litters of newborn offspring from the mating of heterozygous knockout mice (*Mocs1*<sup>+/-</sup>) were injected into the liver with  $1 \times 10^9$  tu of either AAV-MOCS1 or AAV-EGFP at age 1 d. After identification of homozygous knockout mice (*Mocs1*<sup>-/-</sup>) by genotyping, these mice were reinjected with  $4 \times 10^9$  tu of the corresponding virus preparation at age 4 d. Whereas the AAV-EGFP-injected homozygous knockout mice ( $n = 10$ ) showed the typical pathological phenotype and died after an average life span of 8.4 d (fig. 2*a*), only 4 of the 9 AAV-MOCS1-injected homozygous knockout animals ( $n = 9$ ) have died so far (at ages 50 d, 118 d, 124 d, and 137 d). Autopsy of the deceased animals revealed obstructed kidneys as the most probable cause of death. Because of the short half-life of restored xanthine

dehydrogenase, the animals develop xanthine stones in the kidneys and sometimes have renal failure.<sup>4</sup>

After normal results in the open field test (i.e., locomotion, leaning, rearing, and cleaning), two mice were sacrificed at ages 73 d and 64 d, respectively. As a quantifiable parameter for MoCo biosynthesis, total MPT (fig. 1) content in the liver was measured by the *nit1* mutant reconstitution assay<sup>4</sup> and was ~2% of the wild-type level (not shown). Sulphite oxidase activity in the liver was ~5% of the wild-type level (fig. 2*d*). The only observable organ malformation was, again, of the kidneys, which showed signs of obstruction to a variable extent. The remaining three animals of this series were indistinguishable from their healthy littermates (fig. 4), showed urinary sulphite levels comparable to those of the transgenic mice (50 mg/liter), and, by the time this article was prepared, had reached an average life span of 154 d (fig. 2*a*). No offspring were obtained from matings between animals of

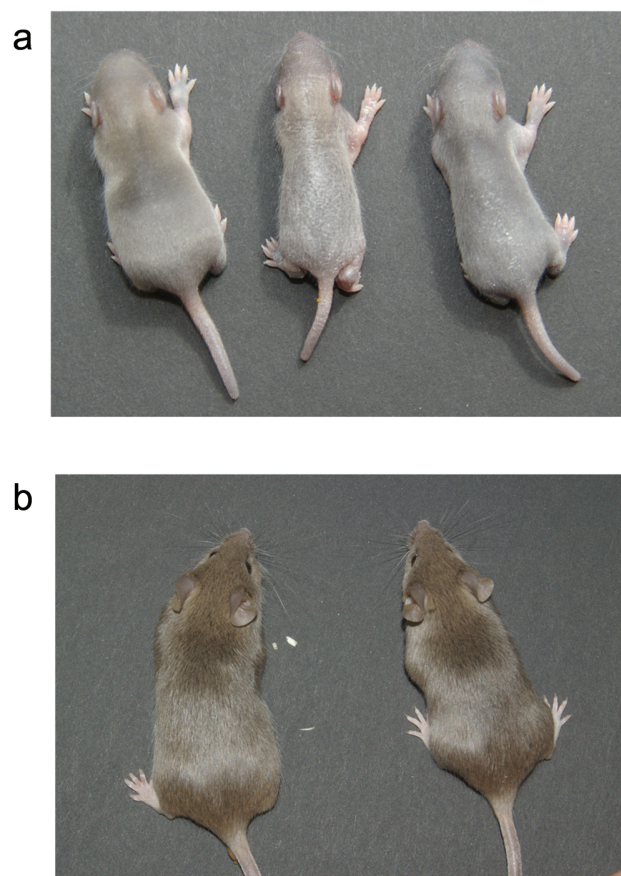


**Figure 4.** Phenotype of homozygous *Mocs1*-deficient mice after AAV-MOCS1 treatment. *a*, Unaffected heterozygous mouse at age 8 d (left), in comparison with an age-matched AAV-EGFP-injected homozygous *Mocs1*-deficient animal (middle) and a homozygous *Mocs1*-deficient littermate injected with AAV-MOCS1 at ages 1 and 4 d (right). *b*, Same animals (left and right in *a*) at age 66 d (the AAV-EGFP-injected animal died at age 9 d).

this series, which could be explained by either urogenital xanthine obstruction or impaired maternal sulphite clearance.<sup>12</sup>

#### *Treatment of Adolescent Mice with AAV-MOCS1*

*Mocs1*-deficient mice do not survive for >2 wk without treatment.<sup>3</sup> However, regular injections of purified cPMP allow them to reach adulthood, although they show reduced activity between ages 20 d and 40 d. We used *Mocs1*-deficient mice treated with isolated cPMP until age 40 d, as described elsewhere,<sup>4</sup> to elucidate the effect of intrahepatic AAV-MOCS1 injections ( $n = 9$ ) in comparison with AAV-EGFP injections ( $n = 10$ ) after withdrawal of the biochemical substitution therapy with cPMP.

As shown in figure 2*b*, the animals mock injected with AAV-EGFP ( $10^{10}$  tu) died, on average, 11 d after the final cPMP injection. However, only one animal injected with AAV-MOCS1 ( $10^{10}$  tu) died 14 d after the AAV injection (cause of death unknown). Four pairs of the surviving animals were mated, and all four matings were fertile. All offspring ( $n = 82$ ) died at age 1–13 d (average 7.5 d). Since the average life span without treatment is the same,<sup>3</sup> this is indirect evidence that no germline transmission of the vector genome occurred (fig. 2*c*).

Mice injected at 40 d after birth revealed no abnormalities in the open field test, and two of them were sacrificed at 60 and 80 d after AAV-MOCS1 injection. The MPT content in liver tissue was ~50% of the wild-type level, and sulphite oxidase activity was ~75% (fig. 2*d*). Autopsy revealed unobstructed kidneys. At the time this article was prepared, the six remaining animals had reached an average age of 151 d (fig. 2*b*). Urinary sulphite levels are ~50 mg/liter, similar to those of transgenic mice.

## Discussion

To date, human clinical gene-therapy trials for inherited diseases have not been unequivocally successful. Because of serious adverse events, such as in the X-SCID (X-linked severe combined immunodeficiency) trials, some studies using retroviral vehicles have been halted.<sup>5</sup> Whereas the use of AAV vectors for the treatment of hemophilia has been successfully demonstrated in mice and nonhuman primates,<sup>13</sup> human subjects present new difficulties due to the lack of reliable test criteria. Transgene-expression levels were low, and corresponding benefits were difficult to quantitate, which can be explained by the availability of a substitution alternative (FactorIX) and consequent compliance deficits.<sup>14</sup> Further, memory cells created during previous AAV infections might be stimulated selectively and eliminate transduced cells, which present fragments of the viral capsid on their surfaces.<sup>15</sup>

These problems may be negligible in the treatment of MoCo deficiency. Patients with MoCo deficiency are given diagnoses in the first weeks or months of their lives and would probably not have been exposed to natural AAV

infections. Thus, preexisting immunity may not interfere with the gene-transfer approach. We demonstrated here that the subjects with devastating disease can be rescued by a single gene-therapy treatment. Expression levels and duration after AAV-MOCS1 transduction of both neonatal and adolescent mice appear to be sufficient to maintain an asymptomatic phenotype. Moreover, we showed that a nonintegrating vector such as AAV<sup>16,17</sup> has the potential to rescue a young and rapidly growing organism. The observed decrease over time of EGFP expression after transduction of neonatal mice most likely reflects a dilution effect caused by this growth. This dilution also appears to be responsible for the higher mortality of the transduced neonates (fig. 2*a*), as compared with the animals transduced in adolescence (fig. 2*b*). Nonetheless, by the time this article was prepared, the amount of vector genomes delivered appeared to be sufficient to maintain transgene expression in a relevant number of hepatocytes in three of these animals for >5 mo. Furthermore, it can be expected that diffusible cPMP is produced in other transduced tissues (fig. 3*l–3u*), thereby adding to the necessary supply of detoxifying enzymes with their essential cofactor.

We have reported elsewhere that *Mocs1*-deficient mice supplemented with purified cPMP show bilateral kidney obstruction at age 20 d, corresponding to high urinary levels of xanthine.<sup>4</sup> We have also confirmed that the obstructing deposits actually represent crystallized xanthine (data not shown). Deceased or sacrificed animals of the first AAV-MOCS1-treated series (neonatally transduced) showed renal obstruction to various degrees. Mice homozygous for isolated xanthine oxidoreductase (XOR) deficiency are runted and do not live beyond age 6 wk.<sup>18</sup> These observations are in contrast to the course of human xanthinuria type 1 and 2, both of which are characterized by XOR deficiency in combination with normal sulphite oxidase activities. The majority of affected humans are asymptomatic, and renal stones develop only occasionally.<sup>19,20</sup>

We believe that the different courses of human and murine XOR deficiency are due to the much lower pH of murine urine,<sup>21</sup> as compared with human urine, which reduces the solubility of xanthine.<sup>22</sup> This belief is corroborated by the absence of xanthine stones or renal failure in the described cases of human MoCo deficiency,<sup>23</sup> in which the clinical course is indistinguishable from that of isolated sulphite oxidase deficiency.<sup>24</sup>

We therefore speculate that treatment of human MoCo deficiency can focus on the treatment of sulphite oxidase deficiency. The animals treated at age 40 d with AAV-MOCS1 do not show any kidney abnormalities, which explains the almost-complete survival in this series. The timely death of the offspring from these animals indicates that the germline is not affected by this treatment.<sup>25</sup>

It remains to be seen whether the described therapy will allow reversal of the neurological damage that is observed in many patients, sometimes at birth. However, we have

demonstrated that an early treatment can completely suppress the phenotype. A successful application in humans should pave the way for prenatal screening procedures, allowing accelerated intervention. Since the vectors used in this study contain the human rather than the murine *MOCS1* sequence, these constructs could be used for clinical studies without further modification.

## Acknowledgments

We thank Günter Schwarz and Jose Angel Santamaria-Araujo for cPMP and for help in enzyme analysis. This work was supported by Deutsche Forschungsgemeinschaft grant Re768/12 (to S.K. and J.R.).

## Web Resource

The URL for data presented herein is as follows:

Online Mendelian Inheritance in Man (OMIM), <http://www.ncbi.nlm.nih.gov/Omim/> (for MoCo deficiency type A)

## References

- Schwarz G (2005) Molybdenum cofactor biosynthesis and deficiency. *Cell Mol Life Sci* 62:2792–2810
- Reiss J, Johnson JL (2003) Mutations in the molybdenum cofactor biosynthetic genes *MOCS1*, *MOCS2*, and *GEPH*. *Hum Mutat* 21:569–576
- Lee HJ, Adham IM, Schwarz G, Kneussel M, Sass JO, Engel W, Reiss J (2002) Molybdenum cofactor-deficient mice resemble the phenotype of human patients. *Hum Mol Genet* 11:3309–3317
- Schwarz G, Santamaria-Araujo JA, Wolf S, Lee HJ, Adham IM, Grone HJ, Schwegler H, Sass JO, Otte T, Hanzelmann P, et al (2004) Rescue of lethal molybdenum cofactor deficiency by a biosynthetic precursor from *Escherichia coli*. *Hum Mol Genet* 13:1249–1255
- Nienhuis AW, Dunbar CE, Sorrentino BP (2006) Genotoxicity of retroviral integration in hematopoietic cells. *Mol Ther* 13:1031–1049
- Gross-Hardt S, Reiss J (2002) The bicistronic *MOCS1* gene has alternative start codons on two mutually exclusive exons. *Mol Genet Metab* 76:340–343
- Malik JM, Shevtsova Z, Bähr M, Kügler S (2005) Long-term in vivo inhibition of CNS neurodegeneration by Bcl-XL gene transfer. *Mol Ther* 11:373–381
- Shevtsova Z, Malik JM, Michel U, Bähr M, Kügler S (2005) Promoters and serotypes: targeting of adeno-associated virus vectors for gene transfer in the rat central nervous system in vitro and in vivo. *Exp Physiol* 90:53–59
- Hauck B, Chen L, Xiao W (2003) Generation and characterization of chimeric recombinant AAV vectors. *Mol Ther* 7:419–425
- Johnson JL, Wuebbens MM, Mandell R, Shih VE (1989) Molybdenum cofactor biosynthesis in humans: identification of two complementation groups of cofactor-deficient patients and preliminary characterization of a diffusible molybdopterin precursor. *J Clin Invest* 83:897–903
- Garrett RM, Bellissimo DB, Rajagopalan KV (1995) Molecular cloning of human liver sulfite oxidase. *Biochim Biophys Acta* 1262:147–149
- Reiss J, Bonin M, Schwegler H, Sass JO, Garattini E, Wagner S, Lee HJ, Engel W, Riess O, Schwarz G (2005) The pathogenesis of molybdenum cofactor deficiency, its delay by maternal clearance, and its expression pattern in microarray analysis. *Mol Genet Metab* 85:12–20
- Nathwani AC, Gray JT, Ng CY, Zhou J, Spence Y, Waddington SN, Tuddenham EG, Kemball-Cook G, McIntosh J, Boon-Spijker M, et al (2006) Self-complementary adeno-associated virus vectors containing a novel liver-specific human factor IX expression cassette enable highly efficient transduction of murine and nonhuman primate liver. *Blood* 107:2653–2661
- Manno CS, Chew AJ, Hutchison S, Larson PJ, Herzog RW, Arruda VR, Tai SJ, Ragni MV, Thompson A, Ozelo M, et al (2003) AAV-mediated factor IX gene transfer to skeletal muscle in patients with severe hemophilia B. *Blood* 101:2963–2972
- Manno CS, Pierce GF, Arruda VR, Glader B, Ragni M, Rasko JJ, Ozelo MC, Hoots K, Blatt P, Konkle B, et al (2006) Successful transduction of liver in hemophilia by AAV-Factor IX and limitations imposed by the host immune response. *Nat Med* 12:342–347
- McCarty DM, Young SM Jr, Samulski RJ (2004) Integration of adeno-associated virus (AAV) and recombinant AAV vectors. *Annu Rev Genet* 38:819–845
- Tenenbaum L, Lehtonen E, Monahan PE (2003) Evaluation of risks related to the use of adeno-associated virus-based vectors. *Curr Gene Ther* 3:545–565
- Vorbach C, Scriven A, Capecchi MR (2002) The housekeeping gene xanthine oxidoreductase is necessary for milk fat droplet enveloping and secretion: gene sharing in the lactating mammary gland. *Genes Dev* 16:3223–3235
- Ichida K, Matsumura T, Sakuma R, Hosoya T, Nishino T (2001) Mutation of human molybdenum cofactor sulfurase gene is responsible for classical xanthinuria type II. *Biochem Biophys Res Commun* 282:1194–1200
- Yamamoto T, Moriwaki Y, Takahashi S, Tsutsumi Z, Tuneyoshi K, Matsui K, Cheng J, Hada T (2003) Identification of a new point mutation in the human molybdenum cofactor sulfurase gene that is responsible for xanthinuria type II. *Metabolism* 52:1501–1504
- Bihun C, Bauck L (2004) Basic anatomy, physiology, husbandry, and clinical techniques. In: Quesenberry K, Carpenter J (eds) *Ferrets, rabbits and rodents*. WB Saunders, St. Louis, pp 286–298
- Shimo T, Ashizawa N, Matsumoto K, Nakazawa T, Nagata O (2005) Simultaneous treatment with citrate prevents nephropathy induced by FYX-051, a xanthine oxidoreductase inhibitor, in rats. *Toxicol Sci* 87:267–276
- Johnson JL, Rajagopalan KV, Wadman SK (1993) Human molybdenum cofactor deficiency. *Adv Exp Med Biol* 338:373–378
- Rupar CA, Gillett J, Gordon BA, Ramsay DA, Johnson JL, Garrett RM, Rajagopalan KV, Jung JH, Bacheyie GS, Sellers AR (1996) Isolated sulfite oxidase deficiency. *Neuropediatrics* 27:299–304
- Couto L, Parker A, Gordon JW (2004) Direct exposure of mouse spermatozoa to very high concentrations of a serotype-2 adeno-associated virus gene therapy vector fails to lead to germ cell transduction. *Hum Gene Ther* 15:287–291